

Production of a ${}^4_{\Lambda}\text{He}$ hypernucleus in the ${}^4\text{He}(\pi, K)$ reactions revisited

Toru Harada^{1,2,*} and Yoshiharu Hirabayashi³

¹*Center for Physics and Mathematics,
Osaka Electro-Communication University,
Neyagawa, Osaka, 572-8530, Japan*

²*J-PARC Branch, KEK Theory Center,
Institute of Particle and Nuclear Studies,
High Energy Accelerator Research Organization (KEK),
203-1, Shirakata, Tokai, Ibaraki, 319-1106, Japan*

³*Information Initiative Center, Hokkaido University, Sapporo, 060-0811, Japan*

(Dated: May 7, 2019)

Abstract

We investigate theoretically production cross sections of the $J^\pi = 0^+$ ground state of a ${}^4_{\Lambda}\text{He}$ hypernucleus in the ${}^4\text{He}(\pi, K)$ reaction with a distorted-wave impulse approximation using the optimal Fermi-averaged $\pi N \rightarrow K\Lambda$ t matrix. We demonstrate the sensitivity of the production cross sections to the Λ wavefunctions obtained from $3N$ - Λ potentials and to meson distorted waves in eikonal distortions. It is shown that the calculated laboratory cross sections of the 0^+ ground state in ${}^4_{\Lambda}\text{He}$ amount to $d\sigma/d\Omega_{\text{lab}} \simeq 11 \mu\text{b/sr}$ at $p_\pi = 1.05 \text{ GeV}/c$ in the K forward direction because of an advantage of the use of the s-shell target nucleus such as ${}^4\text{He}$. The importance of the recoil effects and the energy dependence of the $\pi N \rightarrow K\Lambda$ cross sections is also discussed.

PACS numbers: 21.80.+a, 24.10.Ht, 27.30.+t, 27.80.+w

Keywords: Hypernuclei, DWIA, Cross section, Recoil effect

*Electronic address: harada@osakac.ac.jp

I. INTRODUCTION

Recently, unexpected short lifetimes of a ${}^3_{\Lambda}\text{H}$ hypernucleus were measured in hypernuclear production of high-energy heavy-ion collisions [1–3]; the world average lifetime of $\tau^{(\text{av})}({}^3_{\Lambda}\text{H}) = 185^{+23}_{-28}$ ps is shorter than the free lifetime $\tau_{\Lambda} = 263.2 \pm 2.0$ ps by about 30%. However, ALICE Collaboration [4] newly reported the result of $\tau({}^3_{\Lambda}\text{H}) = 237^{+33}_{-36}$ ps which is moderately closer to τ_{Λ} . This is one of the most topical issues to study hypernuclear physics [5], and is essential because ${}^3_{\Lambda}\text{H}$ is the lightest hypernucleus which provides valuable information on interacting a Λ hyperon with nucleons [6]. In addition, HypHI Collaboration [1] suggested that the lifetime of a ${}^4_{\Lambda}\text{He}$ hypernucleus $\tau({}^4_{\Lambda}\text{H}) = 140^{+48}_{-33}$ ps is shorter than $\tau({}^4_{\Lambda}\text{H}) = 194^{+28}_{-26}$ ps measured in stopped K^- experiments at KEK [7], whereas theoretical calculations [8, 9] predicted $\tau({}^4_{\Lambda}\text{H}) = 196\text{--}264$ ps which depend on the Λ wavefunctions. To solve the lifetime puzzle, experimental measurements of the ${}^{3,4}_{\Lambda}\text{H}$ lifetime have been planned in (K^-, π^0) and (π^-, K^0) reactions on ${}^{3,4}\text{He}$ targets at J-PARC [10, 11]. Therefore, it is important to investigate theoretically production of $A = 3, 4$ hypernuclei via the (\bar{K}, π) and (π, K) reactions on ${}^{3,4}\text{He}$ targets [12]. Especially, we believe that Λ production studies on the ${}^4\text{He}$ target are useful to settle mysterious problems related to the $A = 4$ hypernuclei [13], e.g., overbinding/underbinding anomaly [14, 15], charge symmetry breaking (CBS) [16, 17], and so on.

Many theoretical studies of hypernuclear spectroscopy have been performed in nuclear (K^-, π^-) , (π^+, K^+) , and (γ, K^+) reactions [13]. Production cross sections of Λ hypernuclear states for each reaction are usually characterized by a specific momentum transfer to a Λ hyperon. The (K^-, π^-) reactions on ${}^4\text{He}$ [18] can produce a Λ substitutional state in ${}^4_{\Lambda}\text{He}$ under recoilless conditions. On the other hand, the (π^+, K^+) reactions on ${}^4\text{He}$ enable us to give large momentum transfers of $q = 300\text{--}500$ MeV/ c [19], populating a Λ stretched state which seems to be disadvantageous to the $0s_N \rightarrow 0s_{\Lambda}$ transition in terms of a momentum matching law [20]; however, the production cross sections of ${}^4_{\Lambda}\text{He}$ via the (π^+, K^+) reaction on ${}^4\text{He}$ were predicted theoretically [21] for the non-mesonic weak decay of ${}^4_{\Lambda}\text{He}$ and ${}^4_{\Lambda}\text{H}$ at J-PARC [22]. Consequently, it is worth revisiting investigation of ${}^4_{\Lambda}\text{He}$ production via the (π, K) reactions on ${}^4\text{He}$ because we have now been achieved a good understanding of the nuclear (π, K) reactions [23].

In this paper, we investigate theoretically the production cross sections of the $J^{\pi} = 0^+$

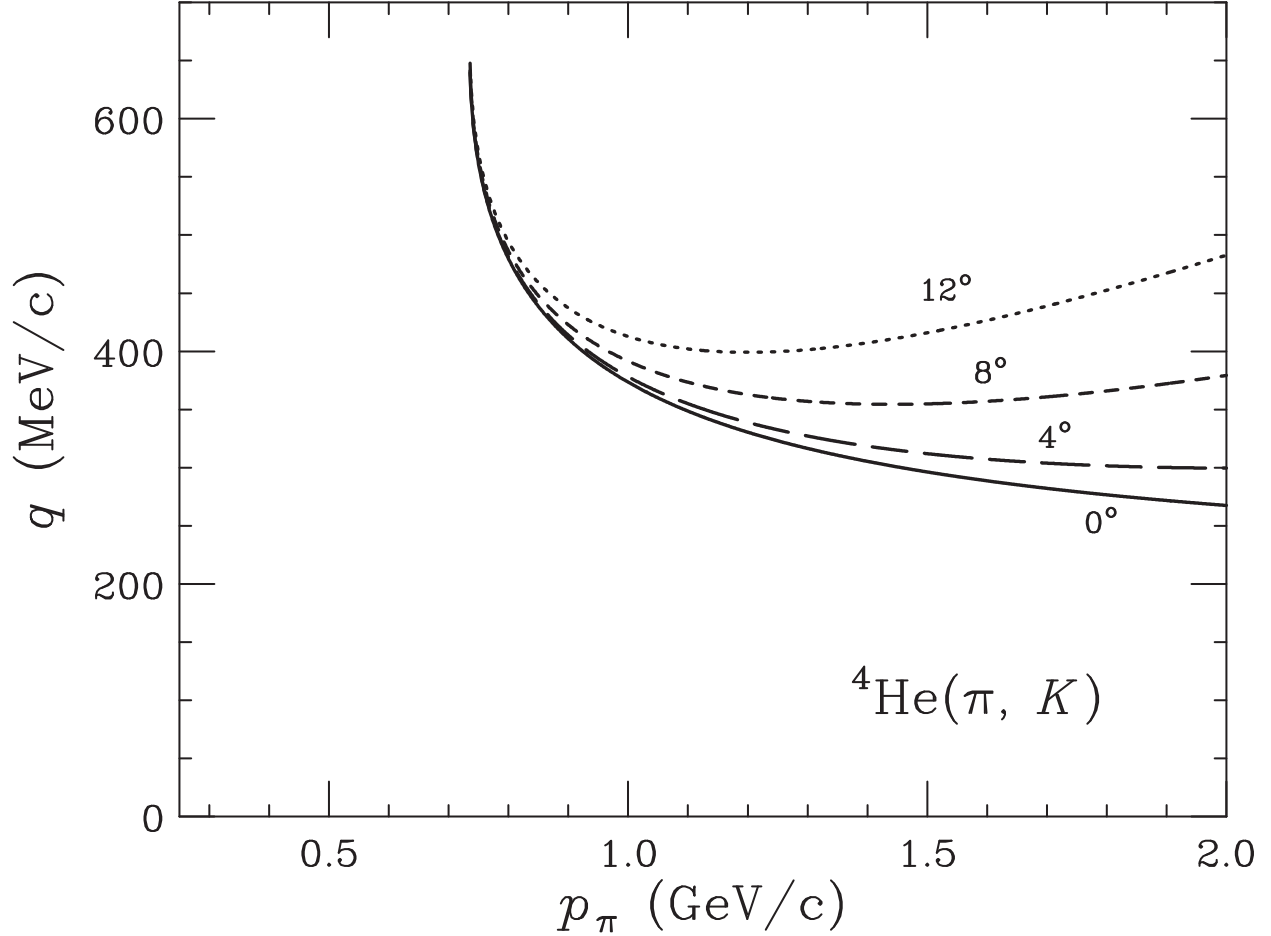


FIG. 1: Momentum transfer q to the Λ final state of $0_{\text{g.s.}}^+$ in ${}^4_{\Lambda}\text{He}$ for (π, K) reactions on a ${}^4\text{He}$ target at K forward-direction angles of $\theta_{\text{lab}} = 0^\circ\text{--}12^\circ$ in the lab frame, as a function of the incident lab momentum p_π .

ground state ($0_{\text{g.s.}}^+$) of a ${}^4_{\Lambda}\text{He}$ hypernucleus via the ${}^4\text{He}(\pi^+, K^+)$ reaction in the distorted-wave impulse approximation. We demonstrate the integrated cross sections at $p_\pi = 1.05$ GeV/c in the K^+ forward direction in the laboratory system. We discuss medium effects of the $\pi N \rightarrow K\Lambda$ amplitude in nuclear (π, K) reactions, and recoil effects in the light hypernucleus such as ${}^4_{\Lambda}\text{He}$. Our results on ${}^4_{\Lambda}\text{He}$ production via (π^+, K^+) reactions are expected to be identical to those on ${}^4_{\Lambda}\text{H}$ mirror production via (π^-, K^0) reactions because charge independence guarantees $f_{\pi^+n \rightarrow K^+\Lambda} = -f_{\pi^-p \rightarrow K^0\Lambda}$ in the (π, K) reactions.

II. CALCULATIONS

A. Distorted-wave impulse approximation

Let us consider a calculation procedure of hypernuclear production for nuclear (π , K) reactions in the laboratory (lab) frame. The inclusive differential cross sections within the distorted-wave impulse approximation (DWIA) [24, 25] are given by (in units $\hbar = c = 1$)

$$\frac{d^2\sigma}{dE_K d\Omega_K} = \beta \frac{1}{[J_A]} \sum_{m_A} \sum_{B, m_B} |\langle \Psi_B | \hat{F} | \Psi_A \rangle|^2 \times \delta(E_K + E_B - E_\pi - E_A), \quad (1)$$

where $[J] = 2J + 1$, and E_K , E_π , E_B and E_A are energies of outgoing K , incoming π , hypernuclear states and the target nucleus, respectively. Ψ_B and Ψ_A are wavefunctions of hypernuclear final states and the initial state of the target nucleus, respectively. The kinematical factor β [26, 27] arising from a translation from a two-body meson-nucleon lab system to a meson-nucleus lab system [28] is given by

$$\beta = \left(1 + \frac{E_K^{(0)}}{E_B^{(0)}} \frac{p_K^{(0)} - p_\pi^{(0)} \cos \theta_{\text{lab}}}{p_K^{(0)}} \right) \frac{p_K E_K}{p_K^{(0)} E_K^{(0)}}, \quad (2)$$

where $p_\pi^{(0)}$ and $p_K^{(0)}$ ($E_K^{(0)}$ and $E_B^{(0)}$) are lab momenta of π and K (lab energies of K and Λ) in the two-body $\pi N \rightarrow K\Lambda$ reaction, respectively. Here we considered only the non-spin-flip reaction because we are interested in the cross sections in the K forward direction. Thus an external operator \hat{F} for the associated production $\pi N \rightarrow K\Lambda$ reactions is given by

$$\hat{F} = \int d\mathbf{r} \chi_K^{(-)*}(\mathbf{p}_K, \mathbf{r}) \chi_\pi^{(+)}(\mathbf{p}_\pi, \mathbf{r}) \times \sum_{j=1}^A \bar{f}_{\pi N \rightarrow K\Lambda} \delta(\mathbf{r} - \mathbf{r}_j) \hat{O}_j, \quad (3)$$

where we assume zero-range interaction for the $\pi N \rightarrow K\Lambda$ transitions. Distorted waves of $\chi_K^{(-)*}$ and $\chi_\pi^{(+)}$ are obtained with the help of the eikonal approximation [24]. \hat{O}_j is a baryon operator changing j th nucleon into a Λ hyperon in the nucleus, and \mathbf{r} is the relative coordinate between the mesons and the center-of-mass (c.m.) of the nucleus; $\bar{f}_{\pi N \rightarrow K\Lambda}$ is the Fermi-averaged amplitude for the $\pi N \rightarrow K\Lambda$ reactions in nuclei on the lab frame [23].

The energy and momentum transfer to the Λ final state is given by

$$\omega = E_\pi - E_K, \quad \mathbf{q} = \mathbf{p}_\pi - \mathbf{p}_K, \quad (4)$$

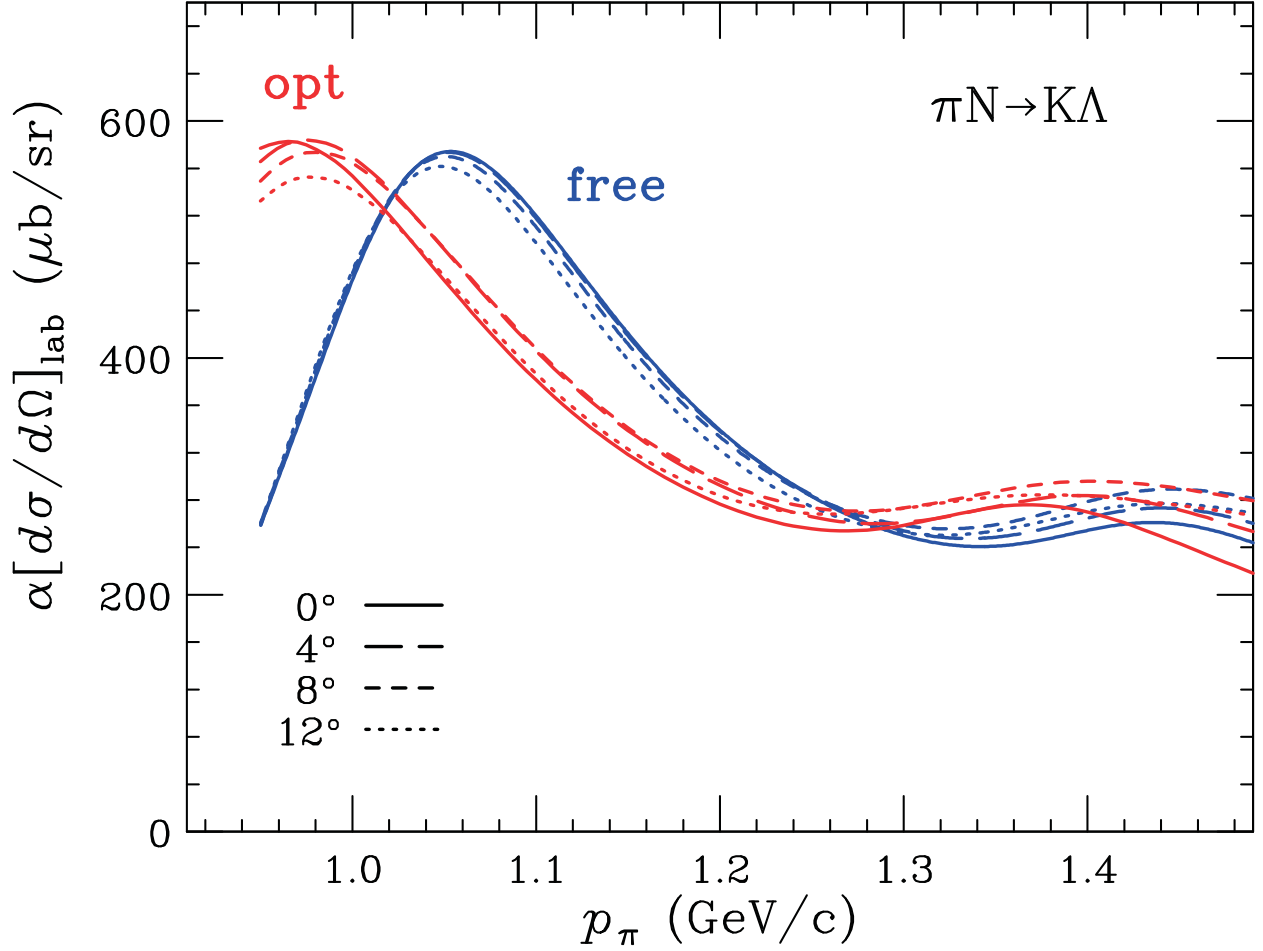


FIG. 2: Optimal Fermi-averaged $\pi N \rightarrow K \Lambda$ lab cross sections of $\alpha \langle d\sigma/d\Omega_K \rangle_{\pi N \rightarrow K \Lambda}^{\text{opt}}$ for the nuclear (π , K) reactions in nuclei [23], as a function of the incident lab momentum p_π . The kinematics for a ${}^4\text{He}$ target at K forward-direction lab angles of θ_{lab} are used. The elementary $\pi N \rightarrow K \Lambda$ lab cross sections of $\alpha \langle d\sigma/d\Omega_K \rangle_{\pi N \rightarrow K \Lambda}^{\text{free}}$ in free space [31] are also drawn.

where $E_\pi = (m_\pi^2 + \mathbf{p}_\pi^2)^{1/2}$ and $E_K = (m_K^2 + \mathbf{p}_K^2)^{1/2}$ are the lab energies of π and K in the nuclear reaction, respectively; m_π and m_K (\mathbf{p}_π and \mathbf{p}_K) are masses (lab momenta) of π and K , respectively. Figure 1 displays the momentum transfer to the $0_{\text{g.s.}}^+$ final state in ${}^4_\Lambda\text{He}$,

$$q = (p_\pi^2 + p_K^2 - 2p_\pi p_K \cos \theta_{\text{lab}})^{1/2}, \quad (5)$$

as a function of the incident lab momentum p_π .

The integrated lab cross section of a Λ hypernuclear state is obtained by the energy

TABLE I: Kinematical values and the $\pi N \rightarrow K\Lambda$ lab cross sections in the nuclear (π, K) reactions on a ${}^4\text{He}$ target at $p_\pi = 1.05 \text{ GeV}/c$.

θ_{lab}	p_K	q	q_{eff}^a	β	α	$\alpha \langle d\sigma/d\Omega \rangle_{\pi N \rightarrow \Lambda K}$	
(degree)	(MeV/c)	(MeV/c)	(MeV/c)			free ($\mu\text{b}/\text{sr}$)	opt ($\mu\text{b}/\text{sr}$)
0	690.1	359.9	271.1	0.684	0.828	574	465
4	689.5	365.4	275.3	0.686	0.829	573	492
8	687.7	381.3	287.3	0.692	0.834	570	492

^aEffective momentum transfer to the Λ final state, $q_{\text{eff}} \approx (M_C/M_A)q$ given in Eq. (26).

integration [29]

$$\left(\frac{d\sigma}{d\Omega_K} \right) = \int dE_K \left(\frac{d^2\sigma}{dE_K d\Omega_K} \right), \quad (6)$$

around a corresponding peak in the inclusive K spectrum. We often adopt the effective number technique into the integrated lab cross section within DWIA [24, 27–30]. Thus the integrated lab cross section of the Λ bound state with J^π can be written as

$$\begin{aligned} \left(\frac{d\sigma}{d\Omega_K} \right)_{\text{lab}, \theta_{\text{lab}}}^{J^\pi} &= \alpha \frac{1}{[J_A]} \sum_{m_A m_B} \left| \left\langle \Psi_B \right| \bar{f}_{\pi N \rightarrow K\Lambda} \right. \\ &\quad \times \chi_K^{(-)*}(\mathbf{p}_K, \frac{M_C}{M_B} \mathbf{r}) \chi_\pi^{(+)}(\mathbf{p}_\pi, \frac{M_C}{M_A} \mathbf{r}) \left. \right| \Psi_A \rangle \Big|^2, \end{aligned} \quad (7)$$

where \mathbf{r} is the relative coordinate between a $3N$ -core nucleus and a nucleon or Λ hyperon; the factors of M_C/M_B and M_C/M_A take into account the recoil effects where M_A , M_B , and M_C are masses of the target, the hypernucleus, and the core nucleus, respectively. The kinematical factor α [28] is related to β in Eq. (2) as

$$\alpha = \beta \left(1 + \frac{E_K p_K - p_\pi \cos \theta_{\text{lab}}}{E_B p_K} \right)^{-1}. \quad (8)$$

In Table I, we show the kinematic values for ${}^4\Lambda\text{He}$ production via the nuclear (π, K) reaction on a ${}^4\text{He}$ target at $p_\pi = 1.05 \text{ GeV}/c$, $\theta_{\text{lab}} = 0^\circ, 4^\circ$, and 8° , where we choose $B_\Lambda = 2.39 \text{ MeV}$ as the Λ binding energy for $0_{\text{g.s.}}^+$ in ${}^4\Lambda\text{He}$. Note that the value of α for a ${}^4\text{He}$ target at $p_\pi = 1.05 \text{ GeV}/c$ (0°) amounts to 0.828 which is 25% larger than that for heavier nuclei; $\alpha \simeq 0.66$ for a ${}^{40}\text{Ca}$ target [20].

B. Fermi-averaged (π , K) cross sections

It should be noticed that the strong energy dependence of differential lab cross sections appears in the nuclear (π , K) reactions, as discussed in Ref. [23]. To consider the p_π dependence of elementary $\pi N \rightarrow K\Lambda$ lab cross sections, we do averaging of the $\pi N \rightarrow K\Lambda$ t matrix in the lab frame over a Fermi-momentum distribution, where nuclear effects of a nucleon binding ε_N are naturally taken into account. This procedure is called as the “optimal Fermi-averaging” under the on-energy-shell condition [23]. Charge independence guarantees the following relation between the $\pi N \rightarrow K\Lambda$ amplitudes:

$$f_{\pi^+n \rightarrow K^+\Lambda} = -f_{\pi^-p \rightarrow K^0\Lambda}. \quad (9)$$

Thus the (π^+, K^+) and (π^-, K^0) cross sections are identical to each other. Here we employed the elementary $\pi^-p \rightarrow K^0\Lambda$ amplitudes analyzed by Sotona and Žofka [31].

Figure 2 shows the optimal Fermi-averaged $\pi N \rightarrow K\Lambda$ lab cross sections of $\alpha\langle d\sigma/d\Omega \rangle_{\pi N \rightarrow K\Lambda}^{\text{opt}}$ including the kinematical factor α in nuclear (π , K) reactions on a ^4He target, together with the elementary $\pi N \rightarrow K\Lambda$ lab cross sections of $\alpha\langle d\sigma/d\Omega \rangle_{\pi N \rightarrow K\Lambda}^{\text{free}}$ in free space [31]. The peaks of $\alpha\langle d\sigma/d\Omega \rangle_{\pi N \rightarrow K\Lambda}^{\text{free}}$ are located at $p_\pi \simeq 1.05$ GeV/ c corresponding to $M(\pi N) \simeq 1700$ MeV/ c^2 in the invariant mass of π and N because there exist N^* resonances, e.g., $S_{11}(1680)$, $P_{11}(1730)$, and $P_{13}(1700)$. We find that the peaks of $\alpha\langle d\sigma/d\Omega \rangle_{\pi N \rightarrow K\Lambda}^{\text{opt}}$ are shifted to the position of $p_\pi \simeq 1.00$ GeV/ c , taken into account the Fermi motion of a struck nucleon under the optimal condition in the nucleus; the shape of $\alpha\langle d\sigma/d\Omega \rangle_{\pi N \rightarrow K\Lambda}^{\text{opt}}$ is moderately broader than that of $\alpha\langle d\sigma/d\Omega \rangle_{\pi N \rightarrow K\Lambda}^{\text{free}}$. In Table I, we also show the values of $\alpha\langle d\sigma/d\Omega \rangle_{\pi N \rightarrow \Lambda K}^{\text{opt}}$, together with the kinematical factor α at $p_\pi = 1.05$ GeV/ c .

C. Wavefunctions

In our calculations, we have assumed the $3N$ $1/2^+$ ground state as a core-nucleus in $A = 4$ systems [18], i.e., ϕ_{3N} is a wavefunction for the $3N$ eigenstates (^3He or ^3H). Thus the wavefunction of the 0^+ ground state in ^4He ($L_A = 0$, $S_A = 0$, $T_A = 0$) is written as

$$\begin{aligned} \Psi_A &= \mathcal{A} \left[[\phi_{3N} \otimes \varphi_{\ell_N}^{(N)}]_{L_A} \otimes X_{T_A, S_A}^A \right]_{J_A}, \\ X_{T_A, S_A}^A &= [\chi_{I_3, S_3}^{(3N)} \otimes \chi_{1/2, 1/2}^{(N)}]_{0,0}, \end{aligned} \quad (10)$$

where \mathcal{A} is the anti-symmetrized operator for nucleons, $\varphi_{\ell_N}^{(N)}$ is a relative wavefunction between $3N$ and N , and X_{T_A, S_A}^A is the isospin-spin function for ${}^4\text{He}$; $\chi_{I_3, S_3}^{(3N)}$ and $\chi_{1/2, 1/2}^{(N)}$ are the isospin-spin functions for $3N$ (isospin I_3 , spin S_3) and N ($I = 1/2$, $S = 1/2$), respectively. The explicit form of X_{T_A, S_A}^A is given in Appendix A. Here we used $\varphi_{\ell_N}^{(N)}$ obtained from the $3N$ - N potential U_N which was derived from a microscopic four-body calculation [32] with a central nucleon-nucleon (NN) potential of Tamagaki's C3G [32]. This potential U_N is parametrized into useful Gaussian forms as

$$U_N(\mathbf{r}) = V_1 \exp\{-(r/b_1)^2\} + V_2 \exp\{-(r/b_2)^2\} + V_3 \exp\{-(r/b_3)^2\} \quad (11)$$

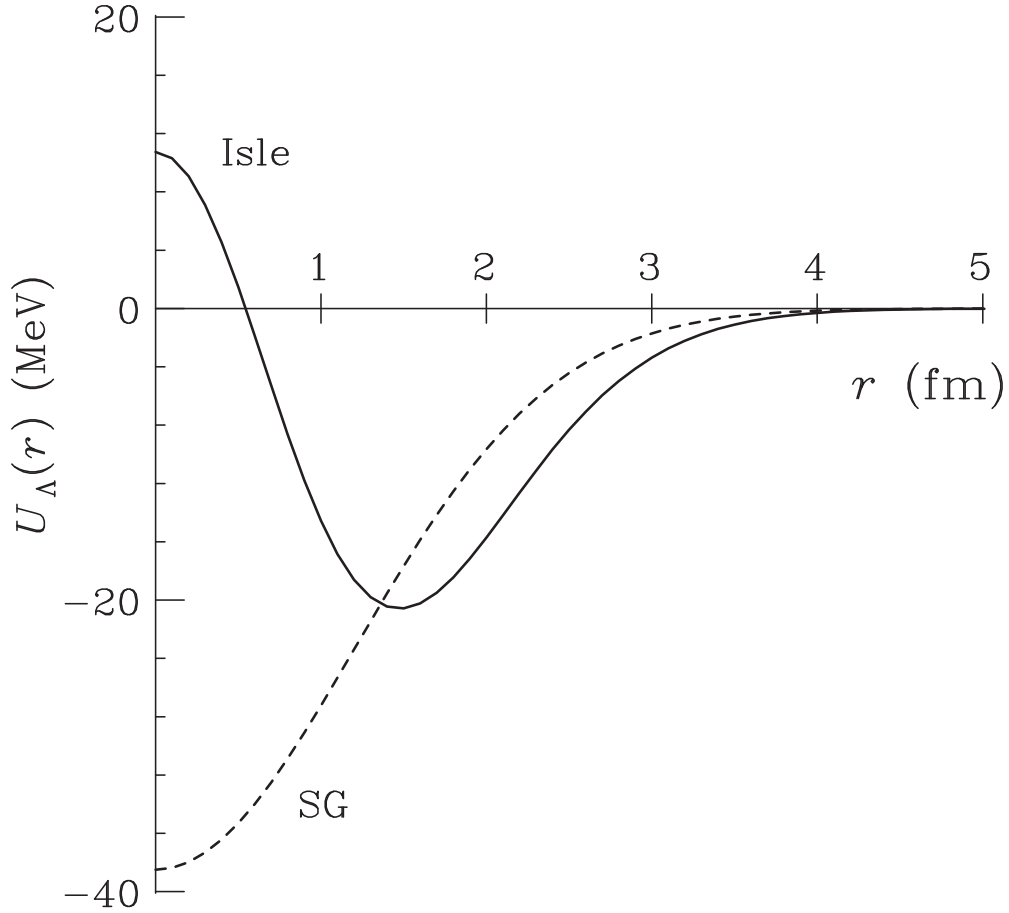


FIG. 3: The $3N$ - Λ potential U_Λ for $0_{\text{g.s.}}^+$ in ${}^4_\Lambda\text{He}$, as a function of the relative distance between $3N$ and Λ . Solid and dash curves denote the Isle and SG potentials, respectively.

with $V_1 = 156.28$ MeV, $V_2 = -185.66$ MeV, $V_3 = -9.56$ MeV, $b_1 = 1.21$ fm, $b_2 = 1.58$ fm, and $b_3 = 2.82$ fm [33], making a fit to the experimental data of the binding energy $B_N = 20.6$ MeV and the nuclear root-mean-square (r.m.s.) distance of $\langle r^2 \rangle^{1/2} = 1.87$ fm between ${}^3\text{He}$ and n .

The wavefunction of the 0^+ ground state ($0_{\text{g.s.}}^+$) in ${}^4\text{He}$ ($L_B = 0$, $S_B = 0$, $T_B = 1/2$) is written as

$$\begin{aligned}\Psi_B &= \left[[\phi_{3N} \otimes \varphi_{\ell_\Lambda}^{(\Lambda)}]_{L_B} \otimes X_{T_B, S_B}^B \right]_{J_B}, \\ X_{T_B, S_B}^B &= [\chi_{I_3, S_3}^{(3N)} \otimes \chi_{0, 1/2}^{(\Lambda)}]_{1/2, 0},\end{aligned}\tag{12}$$

where $\varphi_{\ell_\Lambda}^{(\Lambda)}$ is a relative wavefunction between $3N$ and Λ ; X_{T_B, S_B}^B and $\chi_{0, 1/2}^{(\Lambda)}$ are the isospin functions for $0_{\text{g.s.}}^+$ in ${}^4\text{He}$ and Λ ($I = 0$, $S = 1/2$), respectively. Here we used $\varphi_{\ell_\Lambda}^{(\Lambda)}$ obtained from the $3N$ - Λ potential U_Λ which was derived from a four-body ΛNNN wavefunction based on central NN and ΛN potentials [32, 34]. This potential U_Λ is parameterized into a two-range Gaussian form as

$$\begin{aligned}U_\Lambda(\mathbf{r}) &= V_C \exp\{-(r/b_C)^2\} \\ &\quad + V_A \exp\{-(r/b_A)^2\},\end{aligned}\tag{13}$$

where $V_C = 91.61$ MeV, $V_A = -80.88$ MeV, $b_C = 1.14$ fm, and $b_A = 1.69$ fm, reproducing the experimental data of $B_\Lambda = 2.39 \pm 0.03$ MeV. This potential has a central repulsion and an attractive tail, as shown in Fig. 3, so we call it as “Isle” potential [9, 34, 35]. The central repulsion plays an important role in describing the lifetime of ${}^4\text{He}$ in precise experimental studies on the mesonic weak decay of $\Lambda \rightarrow p\pi^-$ [7, 9]. To clearly see the effect of the central repulsion, we also introduce a single-range Gaussian (SG) potential of $U_\Lambda(\mathbf{r}) = -38.5 \exp\{-(r/b_A)^2\}$ with $b_A = 1.70$ fm, adjusting to $B_\Lambda = 2.39$ MeV. The SG potential is often used as a phenomenological one.

Figure 4 shows that $3N$ - Λ density distributions $\rho_\Lambda(r)$ between $3N$ and Λ for $0_{\text{g.s.}}^+$ in ${}^4\text{He}$, as a function of the relative distance, together with $3N$ - N density distributions $\rho_N(r)$ between $3N$ and N for $0_{\text{g.s.}}^+$ in ${}^4\text{He}$. We find that the $3N$ - Λ distribution obtained from the Isle potential differs fairly from that obtained from the SG potential around the nuclear inside; the $3N$ - Λ distribution is considerably suppressed at the nuclear center, and it is pushed outside, as discussed in Ref. [34, 35]. The relative r.m.s. distance between $3N$ and Λ becomes $\langle r^2 \rangle^{1/2} = 3.57$ fm for Isle, which is 8% larger than 3.31 fm for SG.

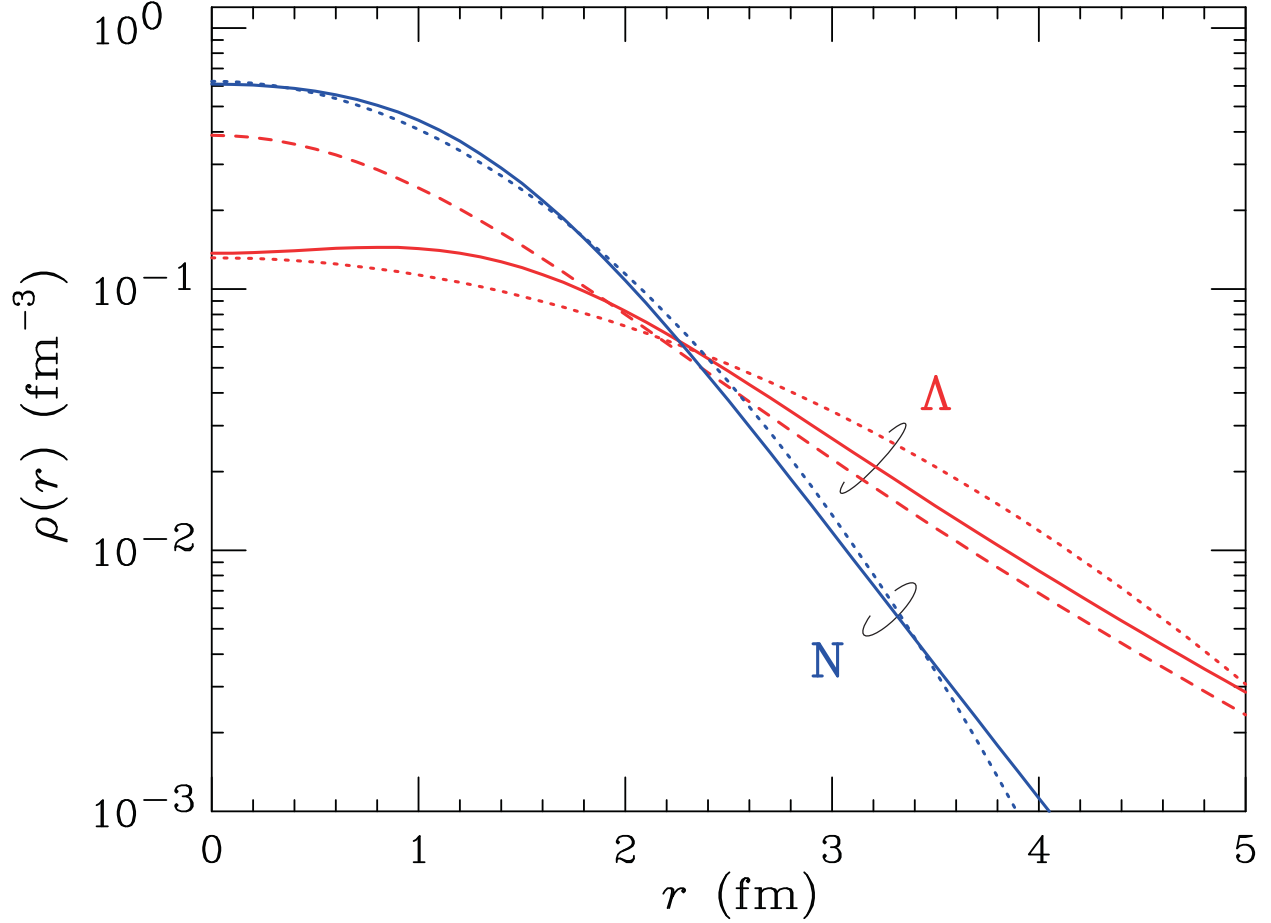


FIG. 4: $3N$ - Λ density distributions $\rho_\Lambda(r)$ for $0_{\text{g.s.}}^+$ in ${}^4_\Lambda\text{He}$, as a function of the relative distance, together with $3N$ - N density distributions $\rho_N(r)$ for $0_{\text{g.s.}}^+$ in ${}^4\text{He}$. Solid and dashed curves for Λ denote the distributions for the Isle and SG potentials, respectively. The solid curve for N denotes the distribution for the C3G potential. Dotted curves are the distributions for HO with the c.m. corrections.

We also consider a single-particle (s.p.) harmonic oscillator (HO) wavefunction with the size parameter $b_\Lambda = (\hbar/m_\Lambda\omega_\Lambda)^{1/2} = 2.233 \text{ fm}$ ($\hbar\omega_\Lambda = 7.0 \text{ MeV}$), which is used as simple model calculations [20, 36]. Figure 4 also shows the $3N$ - Λ distribution for HO taken into account the c.m. correction which is absolutely essential in light nuclei. The size parameter with the c.m. correction denotes

$$\tilde{b}_\Lambda = b_\Lambda \sqrt{1 + m_\Lambda/3m_N}, \quad (14)$$

where m_Λ and m_N are masses of a Λ hyperon and a nucleon, respectively. We find that the

$3N$ - Λ distribution for HO gives $\langle r^2 \rangle^{1/2} = \tilde{b}_\Lambda \sqrt{3/2} = 3.23$ fm where $\tilde{b}_\Lambda = 2.634$ fm, whereas it does not simulate to 3.57 fm for Isle. The difference among the $3N$ - Λ distributions obtained from several models is expected to be clearly observed in production cross sections of nuclear (π, K) reactions giving a large momentum transfer to the Λ final state. On the other hand, we confirm that the $3N$ - N distribution for HO using the size parameter $b_N = 1.329$ fm ($\hbar\omega_\Lambda = 23.5$ MeV) is in good agreement with that obtained from the C3G potential; the relative r.m.s. distance between $3N$ and N has $\langle r^2 \rangle^{1/2} = \tilde{b}_N \sqrt{3/2} = 1.88$ fm which is quite close to 1.87 fm for C3G, where $\tilde{b}_N = b_N \sqrt{4/3} = 1.535$ fm.

D. Integrated cross sections

We consider the integrated lab cross sections of the hypernuclear bound state with J^π on a closed-shell target nucleus with $J_A^\pi = 0_{\text{g.s.}}^+$ like ${}^4\text{He}$, adapting the effective number technique into the DWIA [24, 27–30]. Substituting Eqs. (10), (12), and (23) into Eq. (7), we obtain

$$\left(\frac{d\sigma}{d\Omega_K} \right)_{\text{lab}, \theta_{\text{lab}}}^{J^\pi} = \alpha \left\langle \frac{d\sigma}{d\Omega_K} \right\rangle_{\pi N \rightarrow K\Lambda}^{\text{opt}} N_{\text{eff}}^{J^\pi}(\theta_{\text{lab}}), \quad (15)$$

where $\alpha \langle d\sigma/d\Omega_K \rangle_{\pi N \rightarrow K\Lambda}^{\text{opt}}$ is the optimal Fermi-averaged $\pi N \rightarrow K\Lambda$ lab cross section, as discussed in Sect. II B. The effective number of nucleons $N_{\text{eff}}^{J^\pi}$ for Λ production of the J^π final state in the LS -coupling scheme is written as

$$N_{\text{eff}}^{J^\pi}(\theta_{\text{lab}}) = C_B^2 (2L+1)(2\ell_\Lambda+1) \times \left(\begin{matrix} \ell_\Lambda & L & \ell_N \\ 0 & 0 & 0 \end{matrix} \right)^2 |F(q)|^2, \quad (16)$$

where $\ell_\Lambda + L + \ell_N$ must be even due to the non-spin-flip reaction. Thus, only natural parity states with $J^\pi = 0^+, 1^-, 2^+, 3^-, \dots$ for the $3N + \Lambda$ systems can be populated. C_B is the isospin-spin spectroscopic amplitude between the Λ final state of ${}^4_\Lambda\text{He}$ and the initial state of ${}^4\text{He}$, which is given by

$$C_B = \left\langle X_{T_B, S_B}^B \left| \sum_{j=1}^A \hat{O}_j \right| X_{T_A, S_A}^A \right\rangle. \quad (17)$$

The form factor $F(q)$ in Eq. (16) is given as

$$F(q) = \int_0^\infty r^2 dr \rho_{\ell_\Lambda \ell_N}^{(tr)}(r) \tilde{j}_L(q; \frac{M_C}{M_A} r) \quad (18)$$

with the $N \rightarrow \Lambda$ transition densities

$$\rho_{\ell_\Lambda \ell_N}^{(tr)}(r) = \varphi_{\ell_\Lambda}^{(\Lambda)*}(r) \varphi_{\ell_N}^{(N)}(r) \quad (19)$$

and the distorted waves $\tilde{j}_L(q; z)$ considering the nuclear distortions by mesons in the DW approximation, as we will express in Eq. (24); M_C/M_A is the so-called recoil factor for the momentum transfer q . Here we approximated to $M_C/M_A \approx M_C/M_B$ in Eq. (7). For $J^\pi = 0_{g.s.}^+$ in ${}^4_\Lambda\text{He}$, we take $\ell_\Lambda = \ell_N = L = 0$ and $C_B = \sqrt{2}$ in Eq. (16), then we obtain

$$N_{\text{eff}}^{0+}(\theta_{\text{lab}}) = 2|F(q)|^2, \quad (20)$$

which is expected to observe the hypernuclear fine structure because $F(q)$ is generally sensitive to the nature of the distribution of $\rho_{00}^{(tr)}(r)$, as a function of q .

E. Meson distorted waves

Full distorted waves of the π -nucleus and the K -nucleus are important to reproduce absolute values of the cross sections. Because the (π, K) reaction requires a large momentum transfer with a high angular momentum, we simplify the computational procedure in the eikonal approximation to the distorted waves of the meson-nucleus states [20, 24, 27, 28]:

$$\chi_K^{(-)*}(\mathbf{p}_K, \mathbf{r}) \chi_\pi^{(+)}(\mathbf{p}_\pi, \mathbf{r}) = \exp(i\mathbf{q} \cdot \mathbf{r}) D(\mathbf{b}, z) \quad (21)$$

with

$$D(\mathbf{b}, z) = \exp\left(-\frac{\sigma_\pi(1-i\alpha_\pi)}{2} \int_{-\infty}^z \rho(\mathbf{b}, z') dz' - \frac{\sigma_K(1+i\alpha_K)}{2} \int_z^\infty \rho(\mathbf{b}, z') dz'\right), \quad (22)$$

where σ_π (σ_K) is the averaged total cross section in πN (KN) elastic scatterings, and α_π (α_K) is the ratio of the real and imaginary part of the corresponding forward scattering amplitudes; \mathbf{b} is the impact parameter. $\rho(\mathbf{r}) \equiv \rho(\mathbf{b}, z)$ is a matter-density distribution fitting to the data on the nuclear charge density [37]. We assume $\alpha_\pi = \alpha_K = 0$ which affect hardly the following results, and we study $\sigma_\pi = 20\text{--}30$ mb and $\sigma_K = 10\text{--}30$ mb [20, 24]; $(\sigma_\pi, \sigma_K) = (30 \text{ mb}, 15 \text{ mb})$ is chosen as a standard value [23]. Reducing the r.h.s. in Eq. (21) by partial-wave expansion, we obtain

$$\chi_K^{(-)*}(\mathbf{p}_K, \mathbf{r}) \chi_\pi^{(+)}(\mathbf{p}_\pi, \mathbf{r}) = \sum_L \sqrt{4\pi(2L+1)} i^L \times \tilde{j}_L(q; r) Y_L^0(\hat{\mathbf{r}}) \quad (23)$$

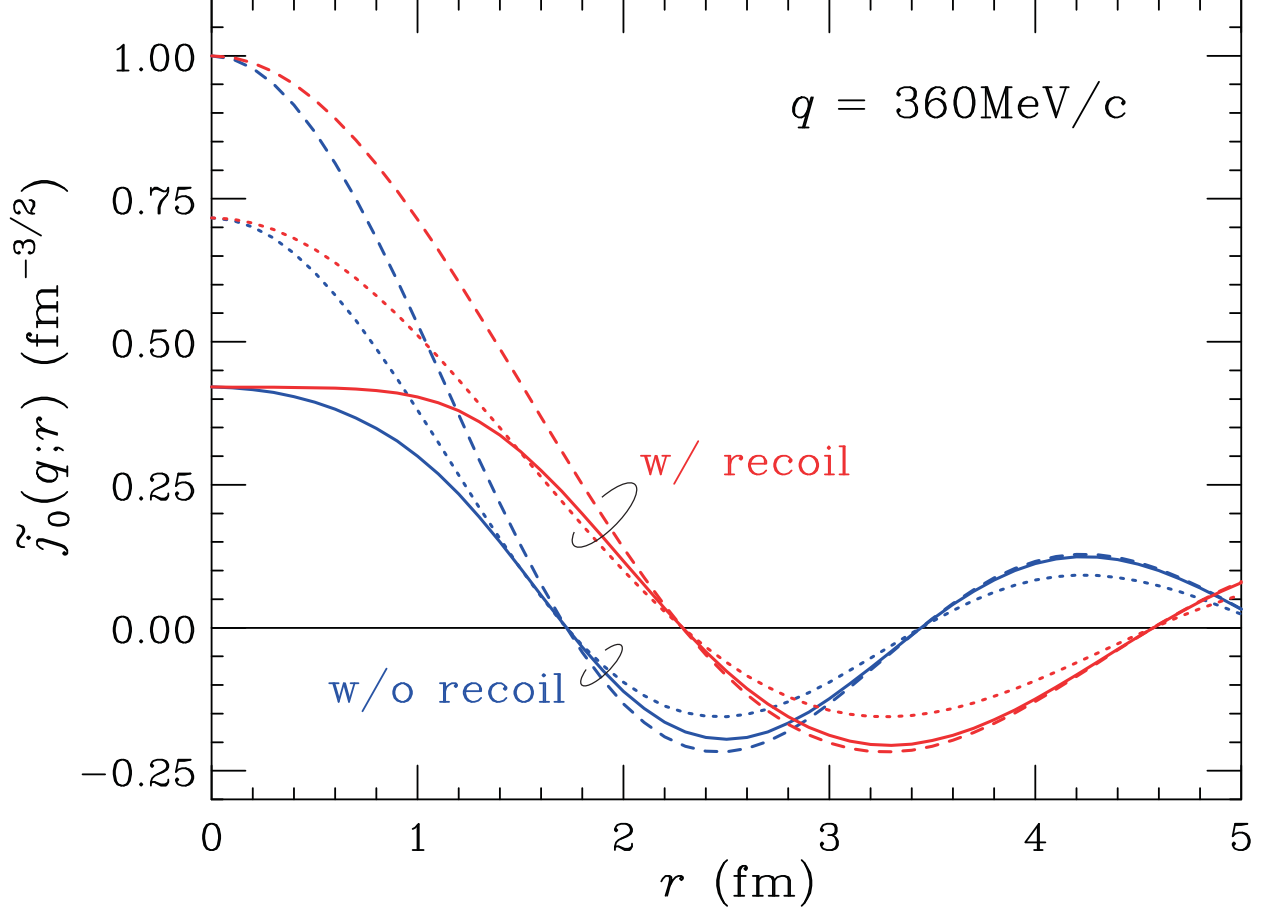


FIG. 5: Distorted waves $\tilde{j}_L(q; r)$ with $L = 0$ for π and K in the ${}^4\text{He}(\pi, K)$ reaction at $p_\pi = 1.05 \text{ GeV}/c$ ($\theta_{\text{lab}} = 0^\circ$) which leads to $q = 360 \text{ MeV}/c$. Solid and dashed curves denote the distorted and the plane waves with/without recoil effects, respectively, as a function of the radial distance between the mesons and the center of the nucleus. Dotted curves denote the waves in the eikonal-oscillator approximation with $\bar{\sigma} = 30 \text{ mb}$.

with

$$\tilde{j}_L(q; r) = \sum_{\ell\ell'} i^{\ell-L} \frac{2\ell+1}{2L+1} \sqrt{2\ell'+1} (\ell 0 \ell' 0 | L 0)^2 \times j_\ell(qr) D_{\ell'}(r), \quad (24)$$

where $D_\ell(r)$ is a distortion function [23] defined as

$$D_\ell(r) = \frac{2\ell+1}{2} \int_{-1}^1 D(\mathbf{b}, z) P_\ell(\cos \theta) d(\cos \theta). \quad (25)$$

Here $z = r \cos \theta$, $\mathbf{r}^2 = \mathbf{b}^2 + z^2$, and $P_\ell(x)$ is a Legendre polynomial. If the distortion is switched off, $\tilde{j}_L(q; r)$ is equal to $j_L(qr)$ which is a spherical Bessel function with L .

Figure 5 displays the distorted waves $\tilde{j}_0(q; r)$ for π and K in the ${}^4\text{He}(\pi, K)$ reactions at $p_\pi = 1.05 \text{ GeV}/c$ ($\theta_{\text{lab}} = 0^\circ$) which leads to $q = 360 \text{ MeV}/c$. We find that the values of $\tilde{j}_0(q; r)$ are reduced near the center of the nucleus due to the nuclear absorption in the distorted wave, in comparison with the plane waves which are obtained with $(\sigma_\pi, \sigma_K) = (0 \text{ mb}, 0 \text{ mb})$. We also find that $\tilde{j}_0(q; r)$ spread outside by taking into account the recoil effects which bring us to use the *effective* momentum transfer

$$\begin{aligned} q_{\text{eff}} &= \frac{M_C}{M_A} q \\ &\simeq \frac{A-1}{A} q = \frac{3}{4} \times 360 = 271 \text{ MeV}/c \end{aligned} \quad (26)$$

in the $A = 4$ hypernuclei, as seen in Table I. We recognize a node in $\tilde{j}_0(q; r)$ at $r = r_n$ satisfied as

$$\frac{M_C}{M_A} q r_n = n\pi, \quad (n = 1, 2, \dots), \quad (27)$$

so we have the point of $r_1 = (M_A/M_C)\pi/q = 2.29 \text{ fm}$ located on the outside of the nucleus having $\langle r^2 \rangle^{1/2} = 1.88 \text{ fm}$ for ${}^4\text{He}$. If we omit the recoil effects ($M_C/M_A \rightarrow 1$), we have $r_1 \rightarrow \pi/q = 1.72 \text{ fm}$ which is located on the inside of the nucleus. Therefore, the recoil effects must be taken into account for the light nuclear target in the (π, K) reactions providing the large momentum transfer to the Λ final state, as we will discuss in Sect. III C.

III. RESULTS AND DISCUSSION

Let us consider the Λ production for $0_{\text{g.s.}}^+$ in ${}^4_\Lambda\text{He}$ via the (π, K) reactions on the ${}^4\text{He}$ target at $p_\pi = 1.05 \text{ GeV}/c$ in the K forward direction. We will discuss the meson distortion effects, comparing between the integrated lab cross sections in PWIA and DWIA, and we will study the sensitivity of the cross sections to the Λ wavefunctions using the effective number technique of Eq. (15).

A. Integrated cross sections for $0_{\text{g.s.}}^+$ in ${}^4_\Lambda\text{He}$

1. PWIA v.s. DWIA

In Table II, we show the calculated PWIA and DWIA results of the integrated lab cross sections for $0_{\text{g.s.}}^+$ in ${}^4_\Lambda\text{He}$ at $p_\pi = 1.05 \text{ GeV}/c$ in the K forward-direction angles of $\theta_{\text{lab}} =$

TABLE II: Calculated PWIA and DWIA results of the integrated lab cross sections of $0_{\text{g.s.}}^+$ in ${}^4_{\Lambda}\text{He}$ via the ${}^4\text{He}(\pi^+, K^+)$ reaction at $p_\pi = 1.05 \text{ GeV}/c$. The Isle, SG, and HO ($\hbar\omega_\Lambda = 7.0 \text{ MeV}$) potentials are used with $(\sigma_\pi, \sigma_K) = (30 \text{ mb}, 15 \text{ mb})$. The recoil effects are taken into account.

θ_{lab} (degree)	$N_{\text{eff}}^{\text{PW}}$ ($\times 10^{-2}$)	$(d\sigma/d\Omega)_{\text{lab}}^{\text{PW}}$ ($\mu\text{b/sr}$)	D_{dis}^a	$N_{\text{eff}}^{\text{DW}}$ ($\times 10^{-2}$)	$(d\sigma/d\Omega)_{\text{lab}}^{\text{DW}}$ ($\mu\text{b/sr}$)
Isle					
0	7.571	35.24	0.334	2.527	11.76
4	6.951	34.18	0.324	2.254	11.08
8	5.390	26.54	0.296	1.595	7.85
SG					
0	12.68	59.01	0.332	4.211	19.60
4	11.82	58.12	0.325	3.841	18.88
8	9.616	47.35	0.303	2.918	14.37
HO					
0	5.539	25.78	0.311	1.724	8.03
4	5.053	24.85	0.300	1.518	7.47
8	3.849	18.95	0.268	1.032	5.08

$$^a D_{\text{dis}} = N_{\text{eff}}^{\text{DW}}/N_{\text{eff}}^{\text{PW}}.$$

$0^\circ\text{--}8^\circ$. The integrated lab cross section of $0_{\text{g.s.}}^+$ in ${}^4_{\Lambda}\text{He}$ accounts for

$$\left(\frac{d\sigma}{d\Omega_K}\right)_{\text{lab},0^\circ}^{J^\pi=0^+} = 35.24 \mu\text{b/sr} \quad (\text{PWIA}) \quad (28)$$

at $p_\pi = 1.05 \text{ GeV}/c$ ($\theta_{\text{lab}} = 0^\circ$), using the Isle potential. When we take into account the distortion with $(\sigma_\pi, \sigma_K) = (30 \text{ mb}, 15 \text{ mb})$, we obtain the integrated lab cross section of $0_{\text{g.s.}}^+$ in ${}^4_{\Lambda}\text{He}$ as

$$\left(\frac{d\sigma}{d\Omega_K}\right)_{\text{lab},0^\circ}^{J^\pi=0^+} = 11.76 \mu\text{b/sr}. \quad (\text{DWIA}) \quad (29)$$

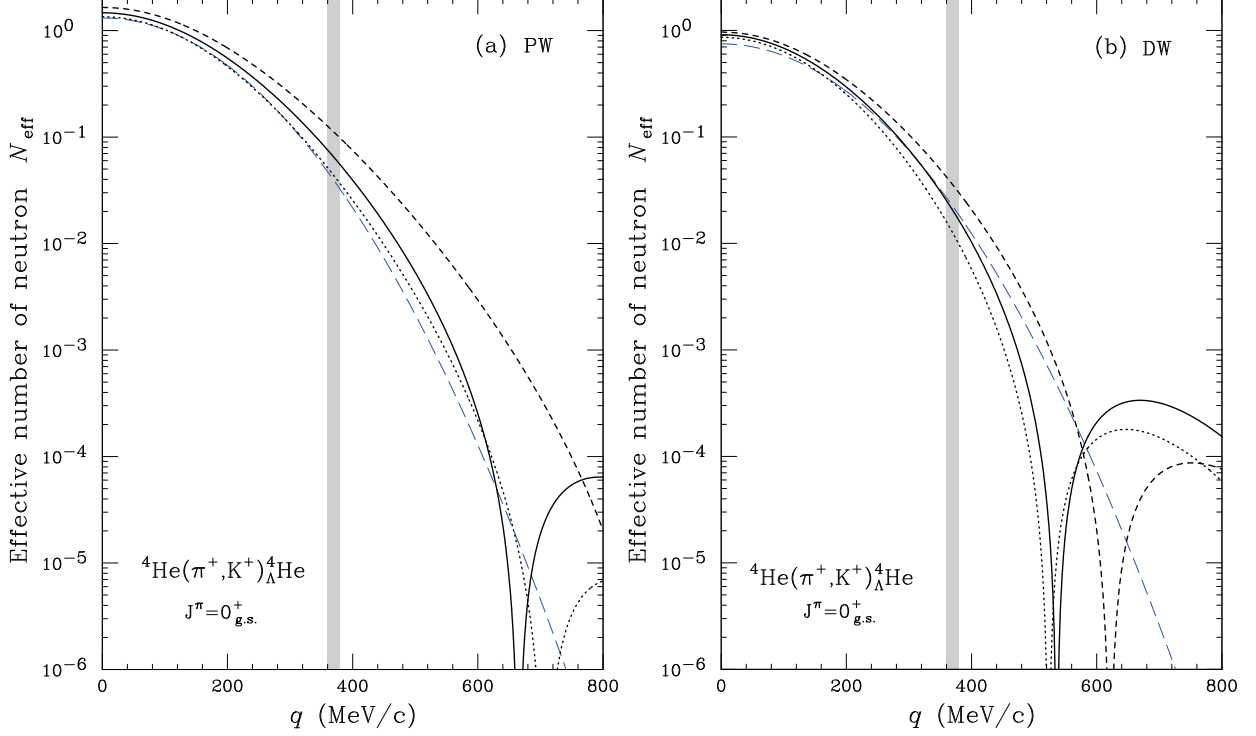


FIG. 6: Calculated effective number of nucleons $N_{\text{eff}}^{0^+_{\text{g.s.}}}$ in ${}^4_{\Lambda}\text{He}$ via the ${}^4\text{He}(\pi^+, K^+){}^4_{\Lambda}\text{He}$ reaction with (a) the plane-wave (PW) and (b) distorted-wave (DW) approximations, as a function of the momentum transfer q . Solid, dashed, and dotted curves denote the results obtained from the Isle, SG, and HO potentials, respectively. Long-dashed curves denote the results in the eikonal-oscillator approximation with $\bar{\sigma} = 30$ mb. The halftones denote the region of $q = 360\text{--}380$ MeV/ c corresponding to $\theta_{\text{lab}} = 0^\circ\text{--}8^\circ$ at $p_\pi = 1.05$ MeV/ c .

We confirm that the integrated lab cross sections in DWIA are relatively reduced by a distortion factor which is defined as

$$D_{\text{dis}} \equiv N_{\text{eff}}^{\text{DW}}/N_{\text{eff}}^{\text{PW}} \simeq 0.3, \quad (30)$$

as shown in Table II. We find that the absolute values of the integrated lab cross sections for SG (HO) are larger (smaller) than those for Isle. This is because the overlaps between wavefunctions between N and Λ are larger inside the nucleus in the order of SG, Isle, and HO, as seen in Fig. 4.

TABLE III: Calculated PWIA and DWIA results of the integrated lab cross sections of $0_{\text{g.s.}}^+$ in ${}^4_{\Lambda}\text{He}$ via the ${}^4\text{He}(\pi^+, K^+)$ reaction at $p_{\pi} = 1.05 \text{ GeV}/c$. The Isle, SG, and HO ($\hbar\omega_{\Lambda} = 7.0 \text{ MeV}$) potentials are used with $(\sigma_{\pi}, \sigma_K) = (30 \text{ mb}, 15 \text{ mb})$. The recoil effects are omitted.

θ_{lab} (degree)	$N_{\text{eff}}^{\text{PW}}$ ($\times 10^{-2}$)	$(d\sigma/d\Omega)_{\text{lab}}^{\text{PW}}$ ($\mu\text{b/sr}$)	D_{dis}	$N_{\text{eff}}^{\text{DW}}$ ($\times 10^{-2}$)	$(d\sigma/d\Omega)_{\text{lab}}^{\text{DW}}$ ($\mu\text{b/sr}$)
Isle					
0	0.886	4.125	0.093	0.082	0.383
4	0.756	3.716	0.077	0.058	0.285
8	0.466	2.292	0.034	0.016	0.077
SG					
0	2.413	11.23	0.162	0.391	1.818
4	2.154	10.59	0.151	0.325	1.597
8	1.538	7.572	0.119	0.183	0.901
HO					
0	0.594	2.765	0.058	0.035	0.161
4	0.507	2.493	0.045	0.023	0.111
8	0.315	1.552	0.012	0.004	0.019

2. N_{eff}^{0+} v.s. q

To see the features of the Λ production of the nuclear (π, K) reactions, we study the effective number of nucleons $N_{\text{eff}}^{J\pi}$, as a function of the momentum transfer q which is determined by the incident lab momentum p_{π} and the K forward-direction angles of θ_{lab} .

Figure 6(a) displays the calculated results of N_{eff}^{0+} , using the Λ wavefunctions obtained from the Isle, SG and HO potentials. The essential physical features of the endothermic nuclear (π, K) reactions can be well understood in terms of N_{eff}^{0+} in PWIA, as suggested by Dover et al. [20]. We confirm that the magnitudes of N_{eff}^{0+} obtained from the SG, Isle, and HO potentials in PWIA are large in this order. Note that the nuclear (π, K) reactions at $p_{\pi} = 1.05 \text{ GeV}/c$ ($\theta_{\text{lab}} = 0^{\circ}\text{--}8^{\circ}$) provide $q = 360\text{--}380 \text{ MeV}/c$ corresponding to the region of the halftones drawn in Fig. 6, where the recoil effects are very important owing to $q_{\text{eff}} \simeq 0.75q$ in

${}^4_\Lambda\text{He}$. On the other hand, exothermic nuclear (\bar{K}, π) reactions with $p_\pi = 0.79 \text{ GeV}/c$ ($\theta_{\text{lab}} = 0^\circ\text{--}8^\circ$) have $q = 68\text{--}126 \text{ MeV}/c$ which denote small momentum transfers, thus the recoil effects do not so affect the integrated lab cross sections. In the region of $q > 600 \text{ MeV}/c$, we find that the values of N_{eff}^{0+} obtained from the Isle potential fall off, and their slopes are steeper than those with the SG potential; a dip appears in the region of $q = 600\text{--}800 \text{ MeV}/c$. This behavior is well known to come from high momentum components in the ΛN and NN wavefunctions due to short-range correlations, as discussed in Ref. [19]. We also find a dip in N_{eff}^{0+} for HO which includes only the NN correlations.

Figure 6(b) shows the calculated results of N_{eff}^{0+} with DWIA. The distortions reduce the magnitudes of N_{eff}^{0+} by about three times (see Table II), changing slightly the shapes of N_{eff}^{0+} in the region of $q < 400 \text{ MeV}/c$. The slopes of N_{eff}^{0+} become gradually steeper as increasing q as in the case of $q > 400 \text{ MeV}/c$, and they grow a dip at the region of $q = 520\text{--}620 \text{ MeV}/c$ which can be achieved by $\theta_{\text{lab}} = 24^\circ\text{--}34^\circ$. These behaviors may originate from high momentum components generated by meson distortions, because $D_0(r)$ significantly modifies $j_0(qr)$ inside the nucleus. Therefore, the distortion effects as well as the recoil effects are very important for large momentum transfer processes which can be realized in the (π, K) reactions.

B. Comparison with eikonal-oscillator approximation

We also consider the integrated lab cross sections using the single-particle (s.p.) harmonic oscillator (HO) wavefunctions and the eikonal distortions by mesons, referring to it as the “eikonal-oscillator” approximation [20]. This is often employed as nuclear model calculations for several reactions [28, 36]. When we use the HO wavefunctions for both nucleon and Λ , we can express the eikonal distorted waves as

$$\chi_K^{(-)*}(\mathbf{p}_K, \mathbf{r})\chi_\pi^{(+)}(\mathbf{p}_\pi, \mathbf{r}) = \exp(iqz) \times \exp\left(-\frac{\bar{\sigma}}{2}T(\mathbf{b})\right) \quad (31)$$

at the K forward direction angle of $\theta_{\text{lab}} = 0^\circ$; the nuclear thickness function is defined as

$$T(\mathbf{b}) \equiv \int_{-\infty}^{\infty} \rho(\mathbf{r})dz, \quad \int T(\mathbf{b})d\mathbf{b} = A, \quad (32)$$

with the averaged total cross section $\bar{\sigma} = (\sigma_\pi + \sigma_K)/2$ for the πN and KN elastic scatterings. Thus we have the effective number of nucleons $N_{\text{eff}}^{J^\pi}$ for $0_{\text{g.s.}}^+$ in Eq. (15), which is rewritten

as [20, 36]

$$N_{\text{eff}}^{0+}(\theta_{\text{lab}}) \simeq 2 \left(\frac{\bar{b}^6}{\tilde{b}_\Lambda^3 \tilde{b}_N^3} \right) \exp \left(-\frac{1}{2} \left(\bar{b} \frac{M_C}{M_A} q \right)^2 \right) \times |G_0(\bar{\sigma})|^2, \quad (33)$$

where the distorted-wave integral [20, 36] is defined by

$$G_0(\bar{\sigma}) = \int_0^\infty 2t \exp(-t^2) \exp \left(-\frac{\bar{\sigma}}{2} T(\bar{b}t) \right) dt, \\ G_0(\bar{\sigma} = 0) = 1. \quad (34)$$

Here the mean HO size parameter denotes

$$1/\bar{b}^2 = (1/\tilde{b}_\Lambda^2 + 1/\tilde{b}_N^2)/2. \quad (35)$$

This formula gives us good insight for the nuclear (π, K) reactions. Figure 6 also displays the values of N_{eff}^{0+} calculated in the eikonal-oscillator approximation of Eq. (33). In the case of PWIA, the magnitude of N_{eff}^{0+} is as large as that obtained from the HO potential, and it is smaller than that obtained from the Isle potential. In the case of DWIA ($\bar{\sigma} = 30$ mb), the magnitude of N_{eff}^{0+} is as large as that for Isle, and these slopes are similar to each other in the region of $q < 400$ MeV/ c . Thus we obtain $(d\sigma/d\Omega)_{\text{lab}}^{\text{DW}} = 12.5, 12.1, \text{ and } 8.8 \mu\text{b/sr}$ at $p_\pi = 1.05$ GeV/ c in $\theta_{\text{lab}} = 0^\circ, 4^\circ, \text{ and } 8^\circ$, respectively; they are comparable to $(d\sigma/d\Omega)_{\text{lab}}^{\text{DW}} = 11.76, 11.08, \text{ and } 7.85 \mu\text{b/sr}$ for Isle. Because high momentum components of neither the N and Λ wavefunctions nor the distorted waves for mesons are included in the eikonal-oscillator approximation, we confirm that the shape of N_{eff}^{0+} has no dip as increasing q .

C. Recoil effects

The recoil effects should be needed in the (π, K) reactions on a very light nuclear target such as ^4He ; the quantity of the recoil factor $M_C/M_A \simeq 3/4 = 0.75$ characterizes the importance of the recoil effects in the nuclear systems. To see the sensitivity to the recoil effects quantitatively, we demonstrate the integrated lab cross sections when we omit the recoil effects ($M_C/M_A \rightarrow 1$) in Eq. (7) using the Isle, SG, and HO potentials.

In Table III, we show the calculated DWIA (PWIA) results of the integrated lab cross sections omitting the recoil effects via the $^4\text{He}(\pi, K)$ reaction at $p_\pi = 1.05$ GeV/ c . We

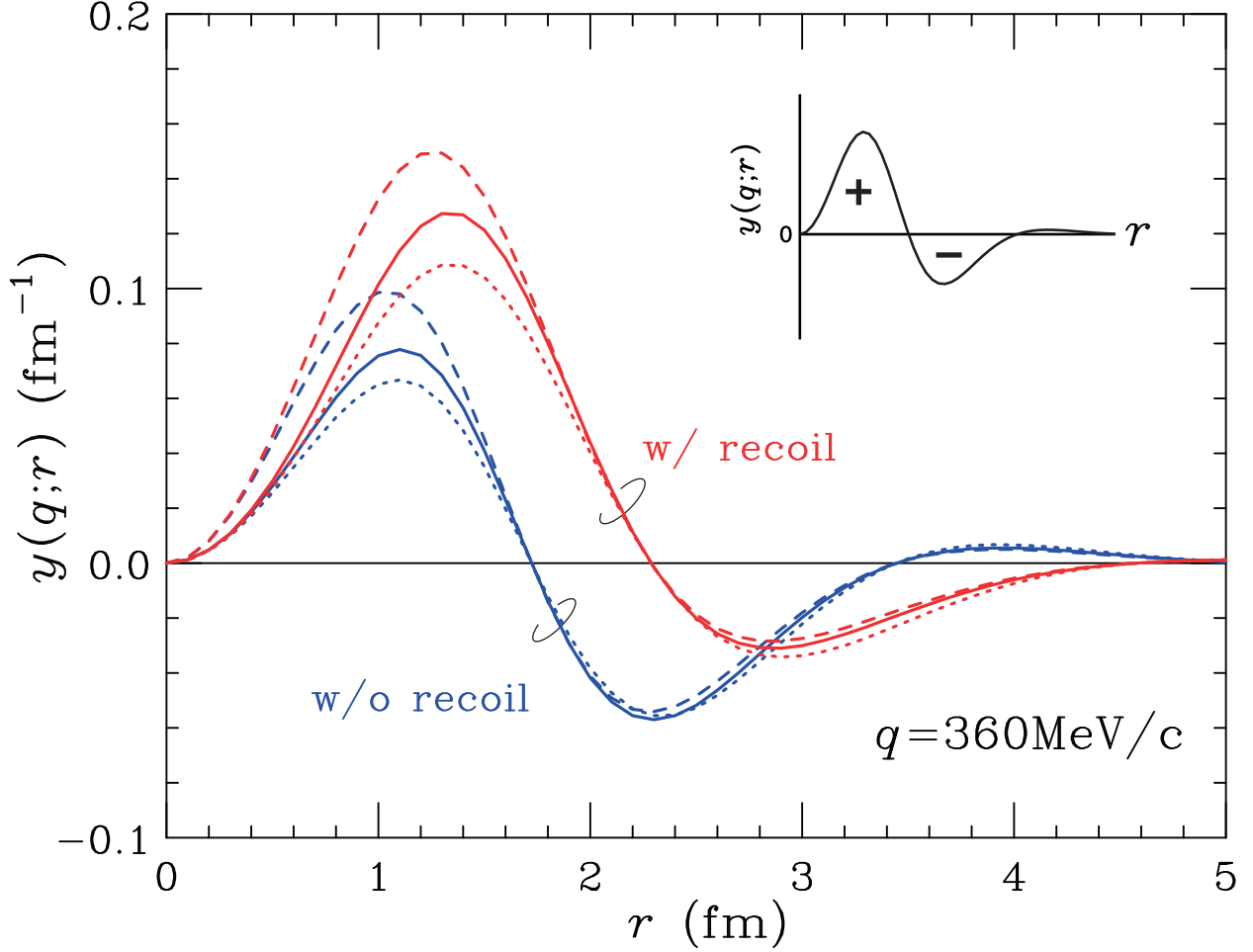


FIG. 7: Overlap functions of $\mathcal{Y}(q; r)$ with/without the recoil effects in the ${}^4\text{He}(\pi, K)$ reactions at $p_\pi = 1.05 \text{ GeV}/c$ (0°) which leads to $q = 360 \text{ MeV}$, as a function of the radial distance. Solid and dashed, dotted curves denote the results obtained from the Isle, SG, and HO potentials, respectively.

find $d\sigma/d\Omega_{\text{lab}} = 0.383 \mu\text{b}/\text{sr}$ ($4.125 \mu\text{b}/\text{sr}$) at $\theta_{\text{lab}} = 0^\circ$. Surprisingly, this value is an order of magnitude smaller than $d\sigma/d\Omega_{\text{lab}} = 11.76 \mu\text{b}/\text{sr}$ ($35.24 \mu\text{b}/\text{sr}$) which is already shown in Table II. The recoil effects have a great influence on $d\sigma/d\Omega_{\text{lab}}$ depending on the radial behavior of the distorted waves for mesons. Here we consider the overlap function defined as

$$\mathcal{Y}(q; r) = r^2 \rho_{00}^{(tr)}(r) \tilde{j}_0(q; \frac{M_C}{M_A} r) \quad (36)$$

which corresponds to the integrand in Eq. (18). Figure 7 displays the behaviors of $\mathcal{Y}(q; r)$ for various types choosing the Λ wavefunctions and the distortion parameters, as a function

of the radial distance. When we omit the recoil effects ($M_C/M_A \rightarrow 1$), we find that the node point at r_1 where $\mathcal{Y}(q; r_1) = 0$ must be shifted toward the nuclear inside. As a result, the integral value of $\int_0^\infty \mathcal{Y}(q; r) dr = F(q)$ is significantly reduced by cancellation between the positive and negative values over integration regions in $\mathcal{Y}(q; r)$, as illustrated in Fig. 7.

The recoil effects are often omitted in several model calculations for nuclear reactions with large momentum transfers, e.g., (π, K) [20], (\bar{K}, K) [28], (\bar{K}, p) [36], and (stopped \bar{K}, π) [38] reactions on ^{12}C in which the recoil effects are not so important because $M_C/M_A \simeq (A-1)/A = 11/12 = 0.917$ for $A = 12$. But we must pay attention to the recoil effects when applying it to light nuclear systems such as ^4He ($M_C/M_A \simeq 3/4 = 0.75$). We believe that the calculated cross sections [28] or calculated production probabilities [38] of $^4_\Lambda\text{He}$ are perhaps underestimated by an order of magnitude for lack of the recoil effects [39].

D. Dependence on distortion parameters

Due to strong absorptions of mesons in nuclei, e.g., π^+ at $p_\pi = 1.0\text{--}1.5$ GeV/ c in the N^* resonance region, the magnitude of the cross section may be also affected by meson distortions. To understand the distortion effects quantitatively, we demonstrate the integrated lab cross sections of $0^+_{\text{g.s.}}$ in $^4_\Lambda\text{He}$, considering various eikonal distortions with parameters of (σ_π, σ_K) . In Table IV, we show the calculated results of $d\sigma/d\Omega_{\text{lab}}$ at $p_\pi = 1.05$ GeV/ c . The magnitudes of the cross sections are reduced as increasing these parameters in DWIA. Thus the integrated lab cross sections of $0^+_{\text{g.s.}}$ in $^4_\Lambda\text{He}$ amount to $(d\sigma/d\Omega)_{\text{lab}} \simeq 8\text{--}14$ $\mu\text{b/sr}$ which depend on π and K distorted waves for $\sigma_\pi = 20\text{--}30$ mb and $\sigma_K = 10\text{--}30$ mb. It should be noticed that the parameter dependence gives an indication of the accuracy of our results within the eikonal distortion. Fully realistic distorted waves obtained from meson-nucleus optical potentials would be needed to make a more quantitative discussion.

E. Dependence on the incident momentum

In Fig. 8, we display the integrated lab cross sections of $0^+_{\text{g.s.}}$ in $^4_\Lambda\text{He}$ via the $^4\text{He}(\pi, K)$ reactions at $\theta_{\text{lab}} = 0^\circ, 4^\circ$, and 8° , as a function of the incident lab momentum p_π . Here we used the Λ wavefunctions obtained from the Isle potential and the eikonal distortions with $(\sigma_\pi, \sigma_K) = (30 \text{ mb}, 15 \text{ mb})$. We find that the integrated lab cross sections slightly increase,

TABLE IV: Distortion-parameter dependence of the integrated lab cross sections of $0_{\text{g.s.}}^+$ in ${}^4_\Lambda\text{He}$ via the ${}^4\text{He}(\pi^+, K^+)$ reaction at $p_\pi = 1.05 \text{ GeV}/c$. The Isle potential for Λ is used.

(σ_π, σ_K) (mb)	θ_{lab} (degree)	D_{dis}	$N_{\text{eff}}^{\text{DW}}$ ($\times 10^{-2}$)	$(d\sigma/d\Omega)_{\text{lab}}^{\text{DW}}$ ($\mu\text{b}/\text{sr}$)
(20, 20)	0	0.387	2.932	13.65
	4	0.378	2.629	12.92
	8	0.351	1.889	9.30
(30, 10)	0	0.372	2.818	13.12
	4	0.363	2.523	12.41
	8	0.335	1.805	8.89
(30, 30)	0	0.243	1.841	8.57
	4	0.234	1.625	7.99
	8	0.206	1.110	5.47

as increasing p_π . This trend seems to be opposite to that of $\alpha\langle d\sigma/d\Omega_{\text{lab}} \rangle_{\pi N \rightarrow K\Lambda}^{\text{opt}}$, as seen in Fig. 2. This comes from the fact that the momentum transfers in this region decrease as increasing p_π (see Fig. 1), together with the nature of $N_{\text{eff}}^{0^+}$ which must be taken into account the recoil effects.

IV. SUMMARY AND CONCLUSION

We have investigated theoretically the production cross sections of the 0^+ ground state of a ${}^4_\Lambda\text{He}$ hypernucleus in the ${}^4\text{He}(\pi, K)$ reaction with a distorted-wave impulse approximation using the optimal Fermi-averaged $\pi N \rightarrow K\Lambda$ t matrix. We have demonstrated the sensitivity of the production cross section to the $3N$ - Λ potentials and to the eikonal distorted waves for mesons. We have calculated the integrated lab cross sections of $d\sigma/d\Omega_{\text{lab}}$ at $p_\pi = 1.05 \text{ GeV}/c$ in the K forward-direction angles of $\theta_{\text{lab}} = 0^\circ$ – 8° . The results can be summarized as follows:

- (1) The calculated integrated lab cross section of $0_{\text{g.s.}}^+$ in ${}^4_\Lambda\text{He}$ amounts to $d\sigma/d\Omega_{\text{lab}} \simeq 11 \mu\text{b}/\text{sr}$ at $p_\pi = 1.05 \text{ GeV}/c$, $\theta_{\text{lab}} = 0^\circ$ – 4° , as in the case of the Isle potential.

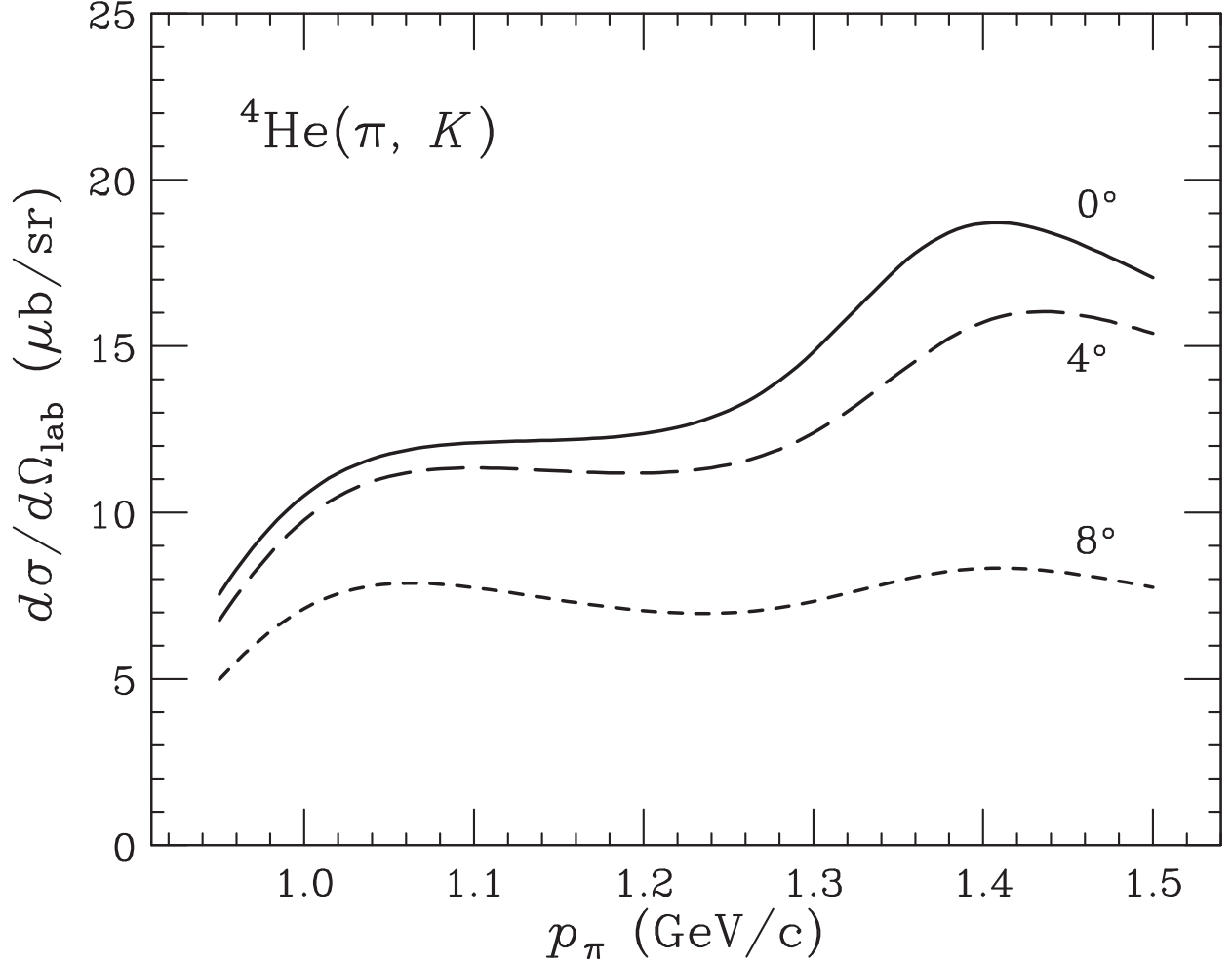


FIG. 8: Incident-momentum dependence of the integrated lab cross sections in the ${}^4\text{He}(\pi, K)$ reactions at $\theta_{\text{lab}} = 0^\circ$, 4° , and 8° , as a function of p_π . The Λ wavefunctions obtained by the Isle potential and the distortion parameters of $(\sigma_\pi, \sigma_K) = (30 \text{ mb}, 15 \text{ mb})$ are used.

- (2) The recoil effects enlarge the cross section of ${}^4_\Lambda\text{He}$ via the ${}^4\text{He}(\pi, K)$ reactions by an order of magnitude, whereas the meson distortions reduce the cross section by 30%.
- (3) It is important to take into account the energy dependence of the $\pi N \rightarrow K\Lambda$ cross sections for a good description of the nuclear (π, K) reactions.
- (4) The integrated lab cross sections of ${}^4_\Lambda\text{H}$ via ${}^4\text{He}(\pi^-, K^0)$ reactions are the same as those of ${}^4_\Lambda\text{He}$ via ${}^4\text{He}(\pi^+, K^+)$ ones owing to charge independence in nuclear physics.

In conclusion, we have shown that the integrated lab cross sections of $0^+_{\text{g.s.}}$ in ${}^4_\Lambda\text{He}$ amount to $d\sigma/d\Omega_{\text{lab}} \simeq 11 \mu\text{b/sr}$ at $p_\pi = 1.05 \text{ GeV}/c$ in the K forward direction because of a major

advantage of the use of the s-shell nuclear targets such as ^4He . It would be appropriate to study the Λ production from the (π, K) reactions on the s-shell $^3,^4\text{He}$ targets in order to study the lifetime measurements of a $^3,^4_\Lambda\text{H}$ hypernucleus in production followed by mesonic decay processes. This investigation is now in progress [12].

Acknowledgments

The authors would like to thank Professor A. Sakaguchi, Professor H. Tamura, and Dr. A. Feliciello for many valuable discussions. This work was supported by Japan Society for the Promotion of Science (JSPS), KAKENHI Grant Numbers JP16K05363.

Appendix A: Explicit forms of isospin-spin functions for $0_{\text{g.s.}}^+$ in ^4He and $^4_\Lambda\text{He}$

The isospin-spin function X_{T_A, S_A}^A for $0_{\text{g.s.}}^+$ in ^4He ($T_A = 0$, $m_{T_A} = 0$; $S_A = 0$, $m_{S_A} = 0$) in Eq. (10) is explicitly written as

$$\begin{aligned}
X_{T_A, S_A}^A &= \mathcal{A}[\chi_{I_3, S_3}^{(3N)} \otimes \chi_{1/2, 1/2}^{(N)}]_{0,0} \\
&= \frac{1}{2\sqrt{6}} \left(-p_\uparrow p_\downarrow n_\uparrow n_\downarrow + p_\uparrow p_\downarrow n_\downarrow n_\uparrow + p_\downarrow p_\uparrow n_\uparrow n_\downarrow \right. \\
&\quad - p_\downarrow p_\uparrow n_\downarrow n_\uparrow + p_\uparrow n_\uparrow p_\downarrow n_\downarrow - p_\uparrow n_\downarrow p_\downarrow n_\uparrow - p_\downarrow n_\uparrow p_\uparrow n_\downarrow \\
&\quad + p_\downarrow n_\downarrow p_\uparrow n_\uparrow - p_\uparrow n_\uparrow n_\downarrow p_\downarrow + p_\uparrow n_\downarrow n_\downarrow p_\uparrow + p_\downarrow n_\uparrow n_\downarrow p_\uparrow \\
&\quad - p_\downarrow n_\downarrow n_\uparrow p_\uparrow - n_\uparrow p_\uparrow p_\downarrow n_\downarrow + n_\uparrow p_\downarrow p_\downarrow n_\uparrow + n_\downarrow p_\uparrow p_\downarrow n_\uparrow \\
&\quad - n_\downarrow p_\downarrow p_\uparrow n_\uparrow + n_\uparrow p_\uparrow n_\downarrow p_\downarrow - n_\uparrow p_\downarrow n_\downarrow p_\uparrow - n_\downarrow p_\uparrow n_\uparrow p_\downarrow \\
&\quad + n_\downarrow p_\downarrow n_\uparrow p_\uparrow - n_\uparrow n_\downarrow p_\uparrow p_\downarrow + n_\uparrow n_\downarrow p_\downarrow p_\uparrow + n_\downarrow n_\uparrow p_\uparrow p_\downarrow \\
&\quad \left. - n_\downarrow n_\uparrow p_\downarrow p_\uparrow \right), \tag{A1}
\end{aligned}$$

where p_\uparrow and n_\uparrow (p_\downarrow and n_\downarrow) denote spin states with $m_z = +1/2$ ($-1/2$) for a proton and a neutron, respectively. The isospin-spin function X_{T_B, S_B}^B for $0_{\text{g.s.}}^+$ in $^4_\Lambda\text{He}$ ($T_B = 1/2$,

$m_{T_B} = +1/2$; $S_B = 0$, $m_{S_B} = 0$) in Eq. (12) is explicitly written as

$$\begin{aligned}
X_{T_B, S_B}^B &= [\chi_{I_3, S_3}^{(3N)} \otimes \chi_{0, 1/2}^{(\Lambda)}]_{1/2, 0} \\
&= \frac{1}{2\sqrt{3}} \big(-p_{\uparrow} p_{\downarrow} n_{\uparrow} \Lambda_{\downarrow} + p_{\uparrow} p_{\downarrow} n_{\downarrow} \Lambda_{\uparrow} + p_{\downarrow} p_{\uparrow} n_{\uparrow} \Lambda_{\downarrow} \\
&\quad - p_{\downarrow} p_{\uparrow} n_{\downarrow} \Lambda_{\uparrow} + p_{\uparrow} n_{\uparrow} p_{\downarrow} \Lambda_{\downarrow} + p_{\downarrow} n_{\downarrow} p_{\uparrow} \Lambda_{\uparrow} - n_{\uparrow} p_{\uparrow} p_{\downarrow} \Lambda_{\downarrow} \\
&\quad + n_{\uparrow} p_{\downarrow} p_{\uparrow} \Lambda_{\downarrow} - n_{\uparrow} p_{\downarrow} p_{\downarrow} \Lambda_{\uparrow} - n_{\downarrow} p_{\uparrow} p_{\uparrow} \Lambda_{\downarrow} + n_{\downarrow} p_{\uparrow} p_{\downarrow} \Lambda_{\uparrow} \\
&\quad - n_{\downarrow} p_{\uparrow} p_{\downarrow} \Lambda_{\uparrow} \big), \tag{A2}
\end{aligned}$$

where Λ_{\uparrow} (Λ_{\downarrow}) denotes a spin state with $m_z = +1/2$ ($-1/2$) for a Λ hyperon.

-
- [1] C. Rappold, et al., HyPHI Collaboration, Nucl. Phys. A **913**, 170 (2013).
 - [2] J. Adam, et al., ALICE Collaboration, Phys. Lett. B **754**, 360 (2016).
 - [3] L. Adamczyk, et al., STAR Collaboration, Phys. Rev. C **97**, 054909 (2018).
 - [4] S. Trogolo, ALICE Collaboration, Nucl. Phys. A **982**, 815 (2019).
 - [5] A. Gal and H. Garcilazo, Phys. Lett. B **791**, 48 (2019), and references therein.
 - [6] H. Kamada, et al., Phys. Rev. C **57**, 1595 (1998).
 - [7] H. Ota, et al., Nucl. Phys. A **639**, 251c (1998).
 - [8] T. Motoba, Nucl. Phys. A **547**, 115 (1992).
 - [9] I. Kumagai-Fuse, S. Okabe, and Y. Akaishi, Phys. Lett. B **345**, 386 (1995).
 - [10] H. Asano, et al., ${}^3\Lambda\text{H}$ and ${}^4\Lambda\text{H}$ mesonic weak decay lifetime measurement with ${}^3,4\text{He}(K^-, \pi^0)_{\Lambda}{}^3,4\text{H}$ reaction, Proposal for Nuclear and Particle Physics experiments at the J-PARC (2018); http://j-parc.jp/NuclPart/Proposal_e.html.
 - [11] M. Agnello, et al., Direct measurement of the ${}^3\Lambda\text{H}$ and ${}^4\Lambda\text{H}$ lifetimes using the ${}^3,4\text{He}(\pi^-, K^0)_{\Lambda}{}^3,4\text{H}$ reactions, Proposal for Nuclear and Particle Physics experiments at the J-PARC (2019); http://j-parc.jp/NuclPart/Proposal_e.html.
 - [12] T. Harada and Y. Hirabayashi, arXiv:1901.03845 [nucl-th].
 - [13] A. Gal, E. V. Hungerford, and D. J. Millener, Rev. Mod. Phys. **88**, 035004 (2016).
 - [14] R. H. Dalitz, R. C. Herndon, and Y. C. Tang, Nucl. Phys. B **47**, 109 (1972).
 - [15] Y. Akaishi, T. Harada, S. Shinmura, Khin Swe Myint, Phys. Rev. Lett. **84**, 3539 (2000).
 - [16] R. H. Dalitz, F. von Hippel, Phys. Lett. **10**, 153 (1964).
 - [17] A. Gal, Phys. Lett. B **744**, 352 (2015); D. Gazda and A. Gal, Nucl. Phys. A **954**, 161 (2016).

- [18] T. Harada, Phys. Rev. Lett. **81**, 5287 (1998); Nucl. Phys. A **672**, 181 (2000).
- [19] S. Shinmura, Y. Akaishi, and H. Tanaka, Prog. Theor. Phys. **76**, 157 (1986).
- [20] C.B. Dover, L. Ludeking, and G.E. Walker, Phys. Rev. C **22**, 2073 (1980).
- [21] T. Harada, unpublished (2006).
- [22] S. Ajimura et al., Exclusive Study on the ΛN Weak Interaction in $A = 4$ Λ -Hypernuclei, Proposal for Nuclear and Particle Physics experiments at the J-PARC (2006); http://j-parc.jp/NuclPart/Proposal_e.html.
- [23] T. Harada and Y. Hirabayashi, Nucl. Phys. A **759**, 143 (2005); **767**, 206 (2006).
- [24] J. Hüfner, S. Y. Lee, and H. A. Weidenmüller, Nucl. Phys. A **234**, 429 (1974).
- [25] E. H. Auerbach, A. J. Baltz, C. B. Dover, A. Gal, S. H. Kahana, L. Ludeking, and D. J. Millener, Ann. Phys. (N.Y.) **148**, 381 (1983).
- [26] S. Tadokoro, H. Kobayashi, and Y. Akaishi, Phys. Rev. C **51**, 2656 (1995).
- [27] T. Koike and T. Harada, Nucl. Phys. A **804**, 231 (2008).
- [28] C. B. Dover and A. Gal, Ann. Phys. (N.Y.) **146**, 309 (1983).
- [29] O. Morimatsu and K. Yazaki, Nucl. Phys. A **483**, 493 (1988); Prog. Part. Nucl. Phys. **33**, 679 (1994).
- [30] K. Itonaga, T. Motoba, O. Richter, and M. Sotona, Phys. Rev. C **49**, 1045 (1994).
- [31] M. Sotona and J. Žofka, Prog. Theor. Phys. **81**, 160 (1989).
- [32] Y. Akaishi, *International Review of Nuclear Physics 4* (World Scientific, Singapore, 1986), p. 259.
- [33] T. Harada, S. Shinmura, Y. Akaishi, and H. Tanaka, Nucl. Phys. A **507**, 715 (1990).
- [34] Y. Kurihara, Y. Akaishi, and H. Tanaka, Prog. Theor. Phys. **67**, 1483 (1982).
- [35] Y. Kurihara, Y. Akaishi, and H. Tanaka, Phys. Rev. C **31**, 971 (1985).
- [36] A. Cieplý, E. Friedman, A. Gal, and J. Mareš, Nucl. Phys. A **696**, 173 (2001).
- [37] H. de Vries, C. W. de Jager, and C. de Vries, At. Data Nucl. Tables **36**, 459 (1987).
- [38] A. Matsuyama and K. Yazaki, Nucl. Phys. A **477**, 673 (1988).
- [39] T. Koike and T. Harada, Phys. Lett. B **652**, 262 (2007).